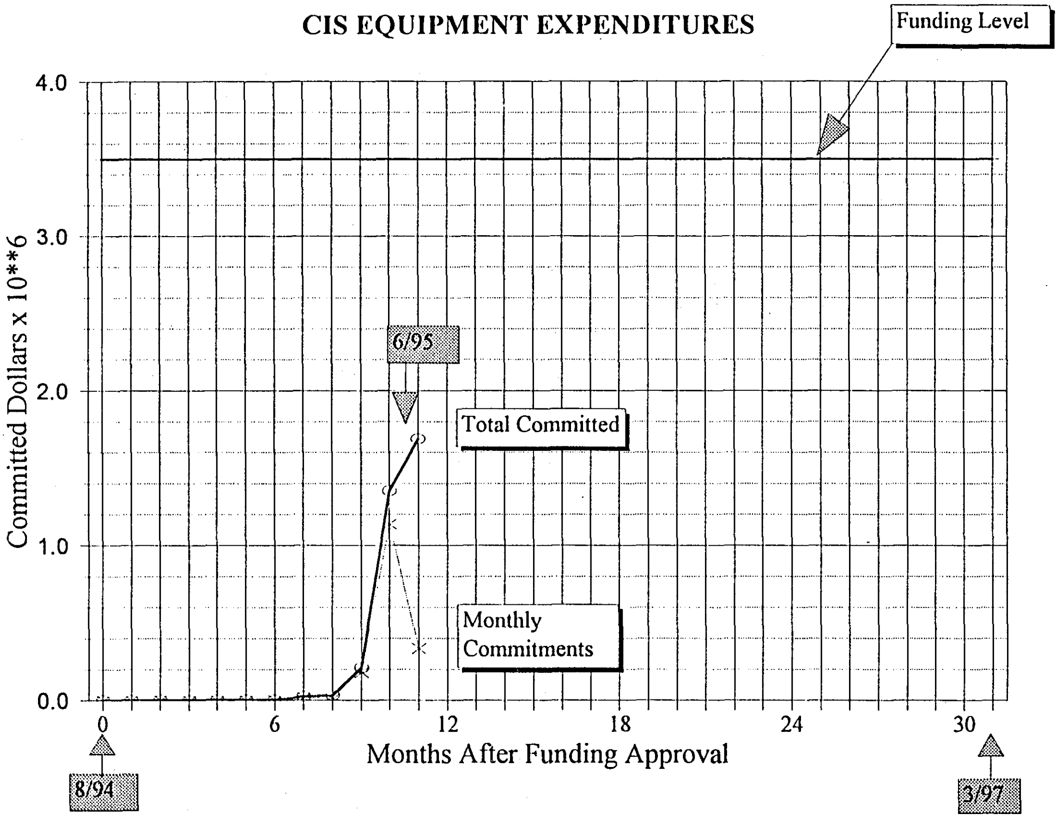

Figure 2. CIS Budget expenditure history.

THE LIGHT ION SPIN SYNCHROTRON (LISS) PROJECT

P. Schwandt
Indiana University Cyclotron Facility, Bloomington, Indiana 47408

I. *The LISS Accelerator Complex*

The principal design goals for LISS are: (1) to accelerate 0.4 GeV polarized protons from the IUCF Cooler ring to maximum energies within the range 10–20 GeV, and other fully-stripped light ions ($A \leq 40$) to corresponding energies (scaled by the charge-to-mass ratio); (2) to accumulate up to $\sim 10^{12}$ particles (corresponding to a circulating current of ~ 0.1A) and store beams for times of order 10^4 s in the absence of internal targets; and (3) to allow for in-ring experiments with internal targets at several long, magnet-free straight sections.

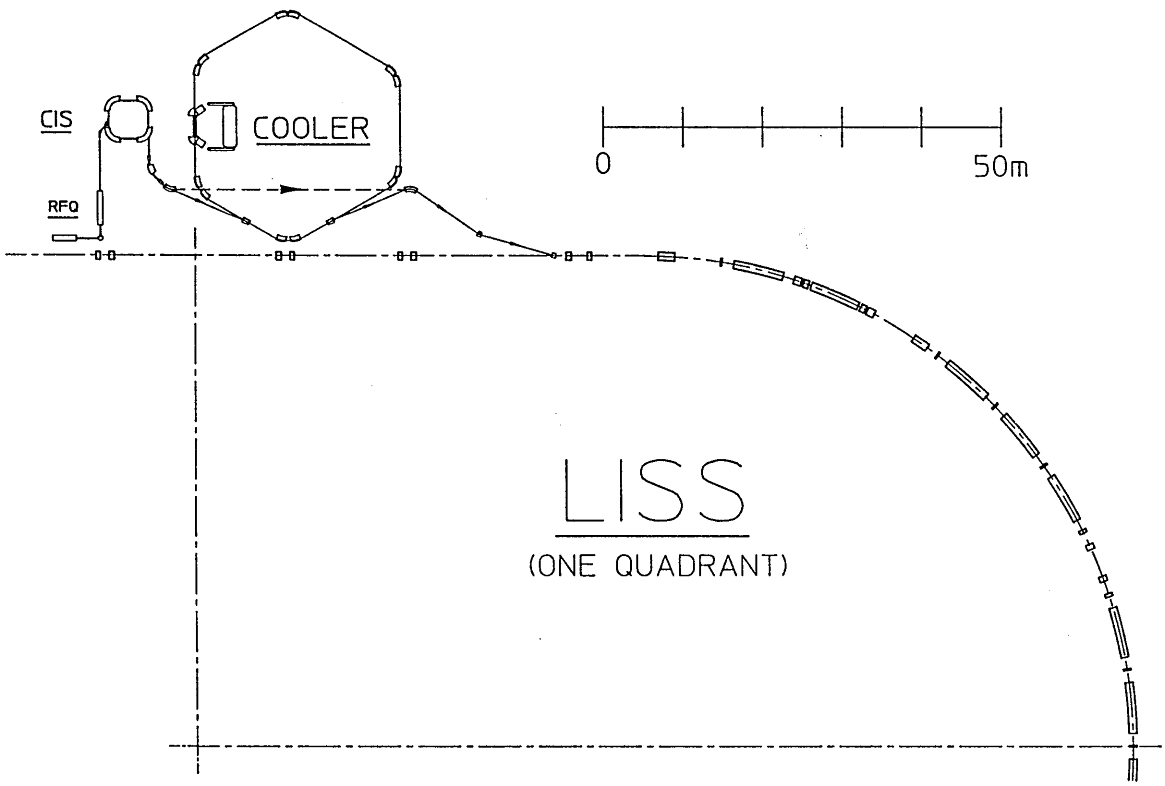

Figure 1. Schematic layout of the proposed CIS-Cooler-LISS accelerator complex.

The total accelerator complex will consist of the new Cooler Injector Synchrotron (CIS) presently under development, the existing 500-MeV Cooler synchrotron/storage ring with electron cooling, and the proposed LISS ring. If the CIS proves capable of accelerating protons to the design energy of 200 MeV, we may consider bypassing the Cooler and inject beam into LISS directly from CIS. Fig. 1 presents a partial layout (to scale) of the proposed CIS–Cooler–LISS accelerator complex.

LISS is conceived as a slow-cycling synchrotron with a 3–5 s acceleration ramp leading to a 16 GeV/c maximum momentum. The racetrack configuration is 608 m in circumference, 7 times the Cooler circumference, with two $>$ 100-m long dispersion-free straight sections with multiple target stations in each. This ring size can be accommodated comfortably on the present IUCF site. A slightly more compact arc lattice design will be studied this summer to see if a 20-GeV/c LISS of 8 times the Cooler circumference is possible.

Assuming for now LISS injection from the Cooler at $\sim$ 0.4 GeV, uncooled (or slightly cooled) beams of moderate transverse emittance ($\geq 1\ \pi$ μm·rad, to keep the incoherent space-charge tune shift below 0.1 at injection) and moderate longitudinal emittance (momentum spread $\Delta p/p \leq 5\times10^{-4}$, to minimize the required RF bucket size in LISS) will be accumulated in LISS. Seven Cooler batches of $\sim 1.5\times10^{11}$ particles each, kick-injected into LISS and captured into RF buckets, would fill LISS to $\sim 10^{12}$ particles. After acceleration to some appropriate energy, say 3–4 GeV, where space charge no longer dominates the beam properties, electron cooling may be used to reduce the beam transverse phase space

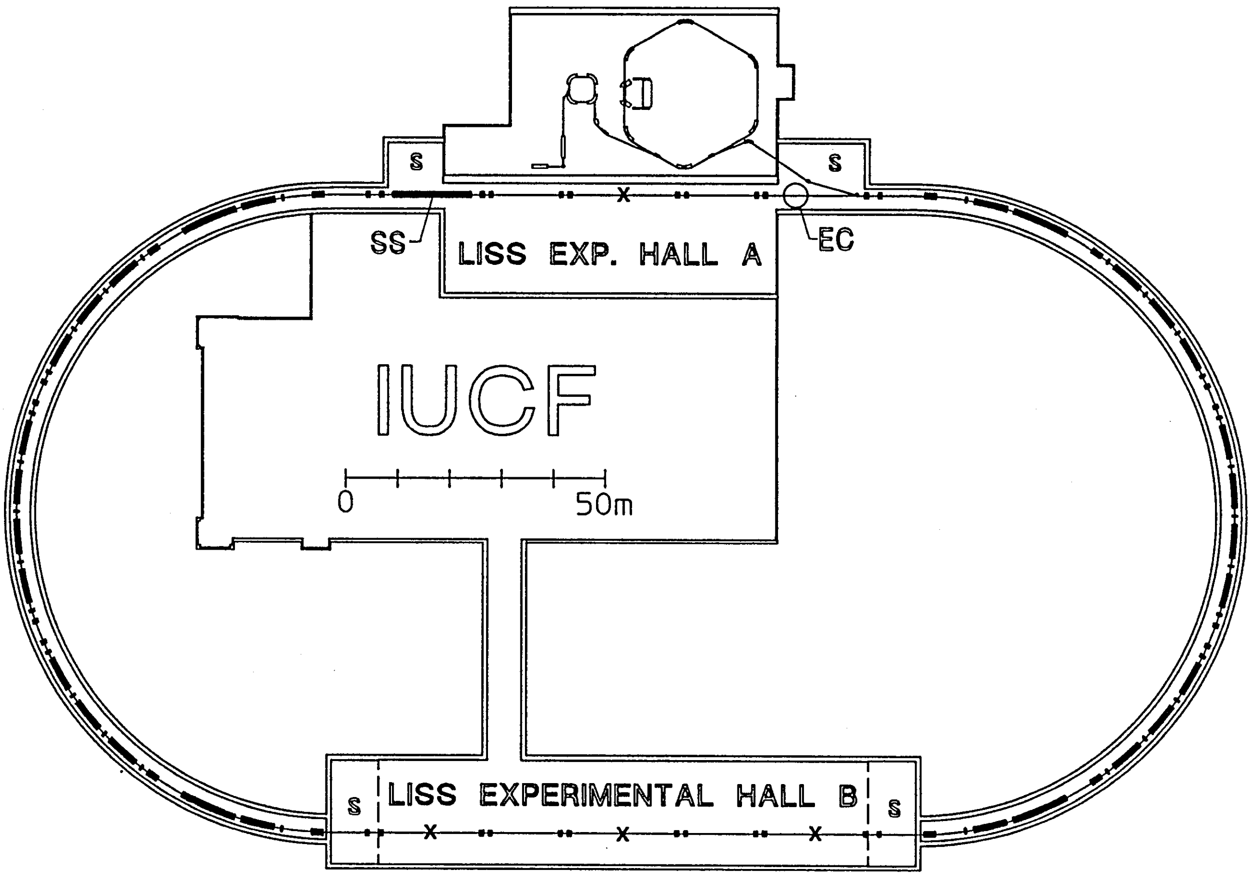

Figure 2. Possible layout of the LISS racetrack on the IUCF site. "X" labels the four principal (low-β) long straight sections available for experiments; "S" denotes Siberian snake(s), "EC" the electron cooling section. Service areas "S" contain utilities distribution centers and magnet power supplies.

significantly in order to benefit high-resolution, low-energy experiments or simply increase the ease of acceleration to high energies. Circulating currents in LISS will be roughly an order of magnitude (or more) lower than in most other operating synchrotrons in the LISS energy range, but beam quality would be considerably higher. The main distinguishing characteristics of LISS are that it is (1) a storage ring for internal-target experiments (which influences its design as an accelerator considerably), possibly incorporating electron cooling, and (2) specifically designed from the outset for acceleration of polarized proton and deuteron beams and providing experimenters with the spin manipulation capabilities for flexible spin orientation and rapid polarization reversals of the stored beam using combinations of Siberian snakes, spin rotators, and RF spin-flip devices.

Figure 2 illustrates a proposed site layout under consideration for the LISS racetrack in relation to the existing IUCF accelerator building and Cooler ring. It has several very useful features in its favor. The accelerator and associated experimental halls are closely coupled to existing facilities. One straight leg of LISS (incorporating Siberian snake(s), the electron-cooling section, and beam injection) would be contained within the existing accelerator building. The ring would occupy the present cyclotron beam corridor, straddled on one side by existing experimental areas (Hall A) and on the other side by the Cooler, thus requiring only a short beam-transfer line. Roughly half of the LISS arc sections are above ground inside a shielding enclosure; the rest are underground. The new experimental Hall B (also underground) is similar to the high-bay area (labelled Exp. Hall A in Fig. 2) in the existing IUCF building, except twice as long.

II. *The LISS Lattice Design*

A prototype, first-order accelerator lattice design for a generic 15-GeV LISS (maximum momentum $p = 16$ GeV/c) has been developed which will form the basis for a more detailed, higher-order beam-dynamics study and conceptual hardware design to be carried out in the course of the next year. The present design is predicated on several very general, desirable characteristics for LISS as both an accelerator and a storage ring for internal-target experiments. The primary criteria are:

- a racetrack configuration to provide experimental bend-free legs, each at least 100 m long;
- at least three low-beta straight sections of about 20-m average free length in each leg as target regions and as locations for spin-manipulation devices (snakes, rotators, flippers), beam injection, beam acceleration, and electron cooling;
- zero dispersion in the long straight sections;
- a very high or imaginary transition energy to avoid transition crossing.

For a given number ($N \geq 6$) of dispersion-free straight sections, a racetrack configuration provides a more flexible and more compact lattice than a ring in the shape of an N-sided polygon.

To avoid instabilities and beam loss due to space-charge effects often encountered in the zero phase-focussing regime when crossing the transition energy, we decided to design an accelerator lattice having an imaginary transition energy (imaginary Lorentz energy factor γ_t), i.e., a *negative* momentum compaction factor $\alpha_c \equiv \gamma_t^{-2}$. In the present design this is achieved by composing each 180° bend arc of the LISS racetrack of a number of compact, basic modules tuned to provide negative momentum compaction α_c. These "Flexible Momentum Compaction" (FMC) lattice modules, proposed recently by S.Y. Lee, *et al.* (Ref. 1), achieve a negative α_c by means of predominantly negative dispersion in the FODO cell dipoles, and a short, straight (dipole-free) optical-function matching section with positive dispersion. The matching section provides a dispersion-closed orbit over the FODO-match-FODO FMC module with no contribution to the momentum compaction factor. The dispersion excursions in the FMC modules can be controlled and minimized to values less than the maximum dispersion of a regular FODO lattice containing the same FODO cells. With the phase advance of the basic module adjusted to $3\pi/2$, and with 4 modules forming each 180°-arc lattice, both the distortion functions of the sextupoles necessary for chromaticity correction, and the systematic half-integer stop band width, are also minimized. Such a lattice is expected to exhibit excellent chromatic properties, should prove very tunable, and provide a dynamic aperture as large as that of a regular FODO lattice.

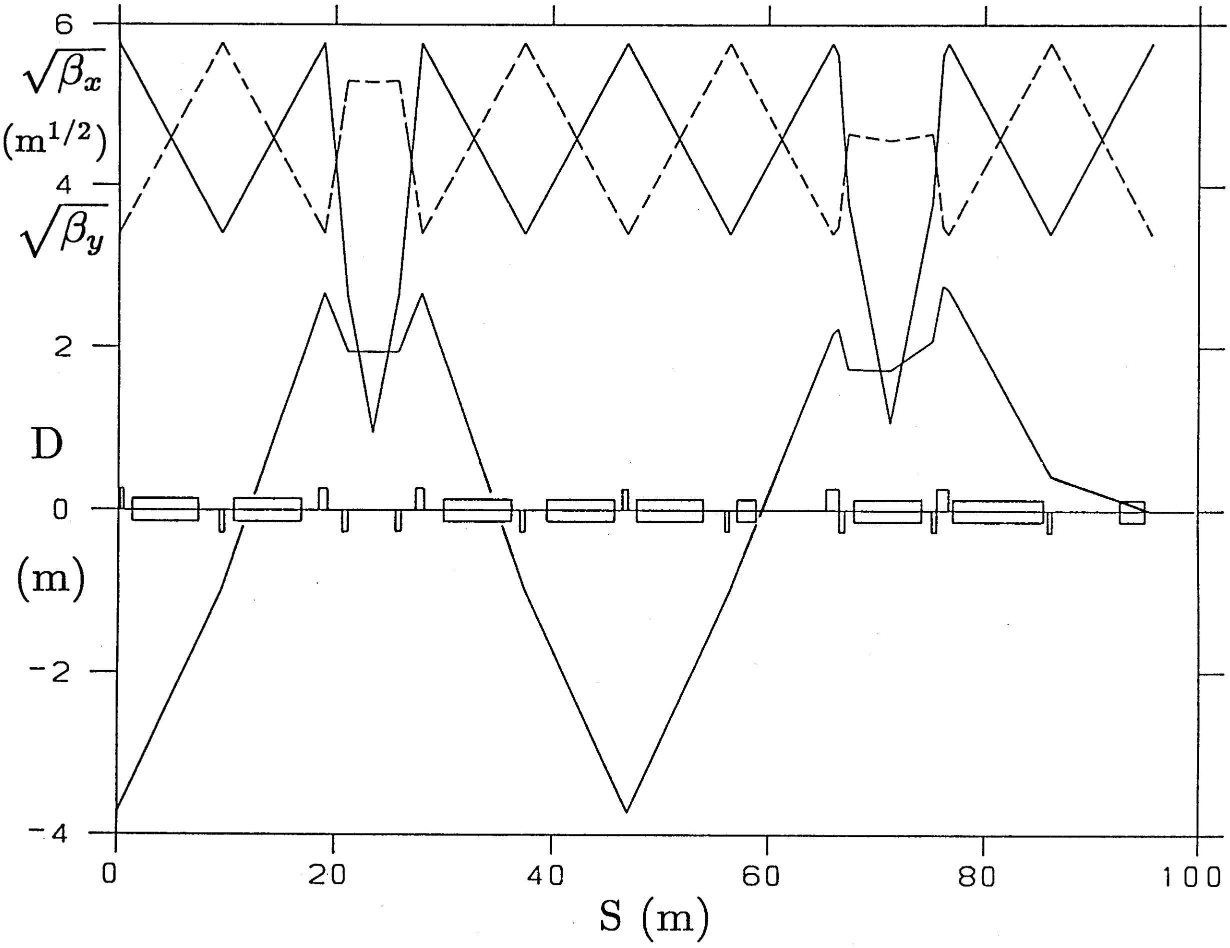

Figure 3. Lattice functions and magnet arrangement for a 90° arc section.

Zero (or very low dispersion) in the long straight sections used for experiments is desirable in many (though by no means all) cases, e.g., when using long, small-aperture storage-cell type gas targets. Zero dispersion D (and zero slope D') at the ends of each arc is achieved in the present lattice design by redistribution of dipoles within the first and last of the FMC arc modules. These D-suppression modules consequently have a small *positive* α_c contribution which, however, is only one quarter of the *negative* α_c contribution from the remaining regular FMC modules in each arc. Hence the arcs overall have a *negative* momentum compaction factor, providing a value of $\gamma_t = 13i$ for the LISS ring.

The lattice for a 90° arc section (arc center to arc exit) with its betatron and dispersion functions is shown in Fig. 3. Both maximum β-functions and D-excursions are acceptably small. The complete ring has betatron tunes $Q_x = 8.16$, $Q_y = 7.20$. The superperiodicity of both the combined (360° bend) arcs, as well as that of the racetrack as a whole, is $P = 2$. (see Fig. 3). The desired total of at least 6 matched, zero-D, low-β straight sections of at least 20-m average clear length can be achieved with a ring circumference of 7 times the IUCF Cooler ring circumference, or 608 m. With an average FMC module length of 47.5 m, each straight leg of the racetrack is then nearly 114 m in length. Fig. 4 shows the

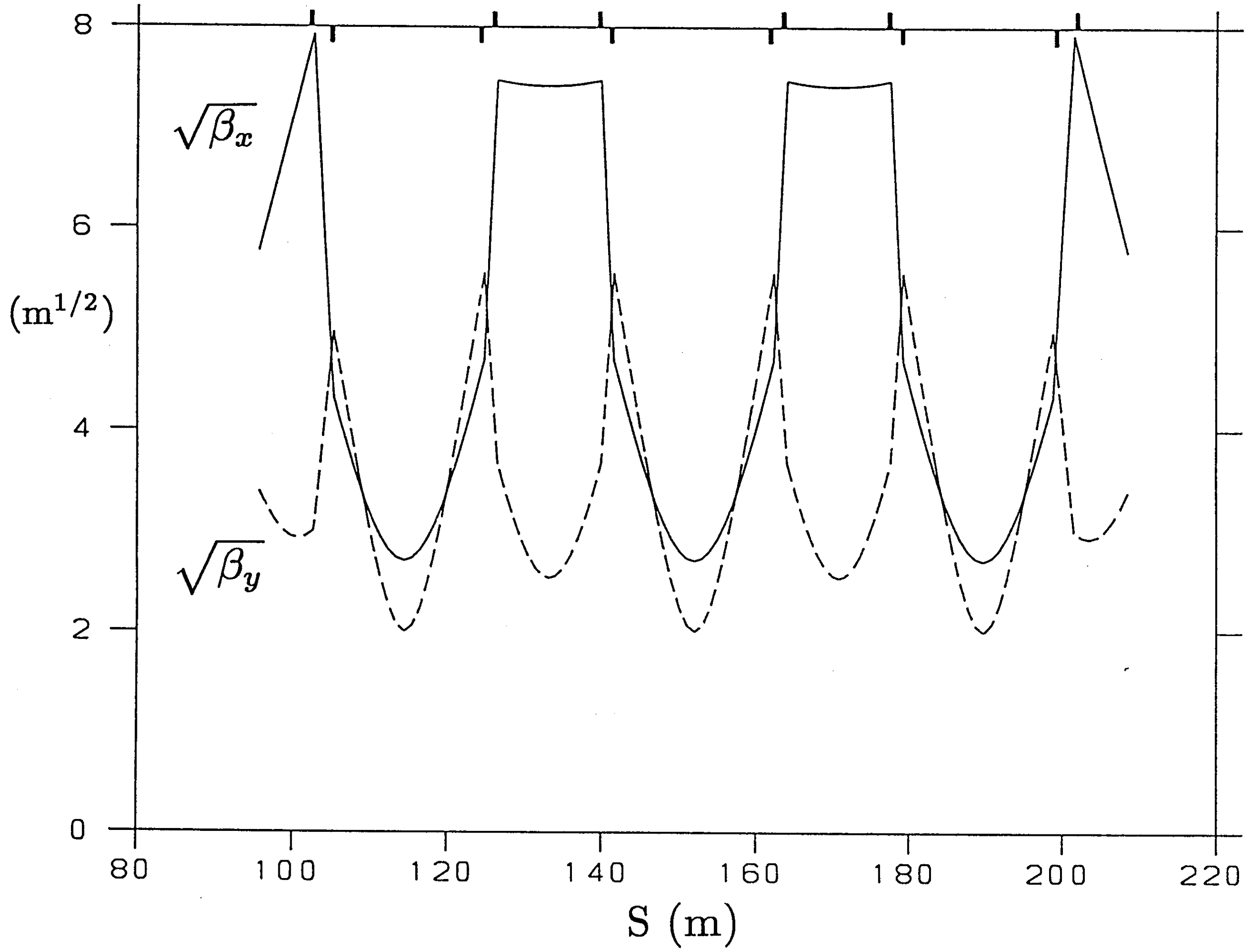

Figure 4. Lattice functions and quadrupole arrangement for one leg of the racetrack straight sections.

focussing lattice and associated β- functions for one possible way of subdividing each leg into straight sections, here 3 identical ones (alternative designs with a mix of longer and shorter sections have also been calculated).

In addition to the 3 identical low-β sections ($\beta^*_{x,y} = 7.5, 5.0$ m) of 20-m clear length, each leg provides two additional matching straight sections of 13-m useful length, each with small β^*_y but large β^*_x. Each straight leg of the racetrack is tuned to $Q_y = 2.0$; the choice of *integer* vertical betatron tune Q_y makes each straight leg "spin-transparent" for beams polarized in the vertical plane. This does not, however, raise the spin periodicity of the ring and hence does not result in a reduction of the number of intrinsic depolarizing spin resonances.

The arcs and the optics-matching sections to the long straight sections also provide a number (up to 8) of potentially useful short straight sections, of 6-7 m usable length, with a variety of lattice function values; some of these will prove useful for various beam-manipulation functions or as short experimental straight sections.

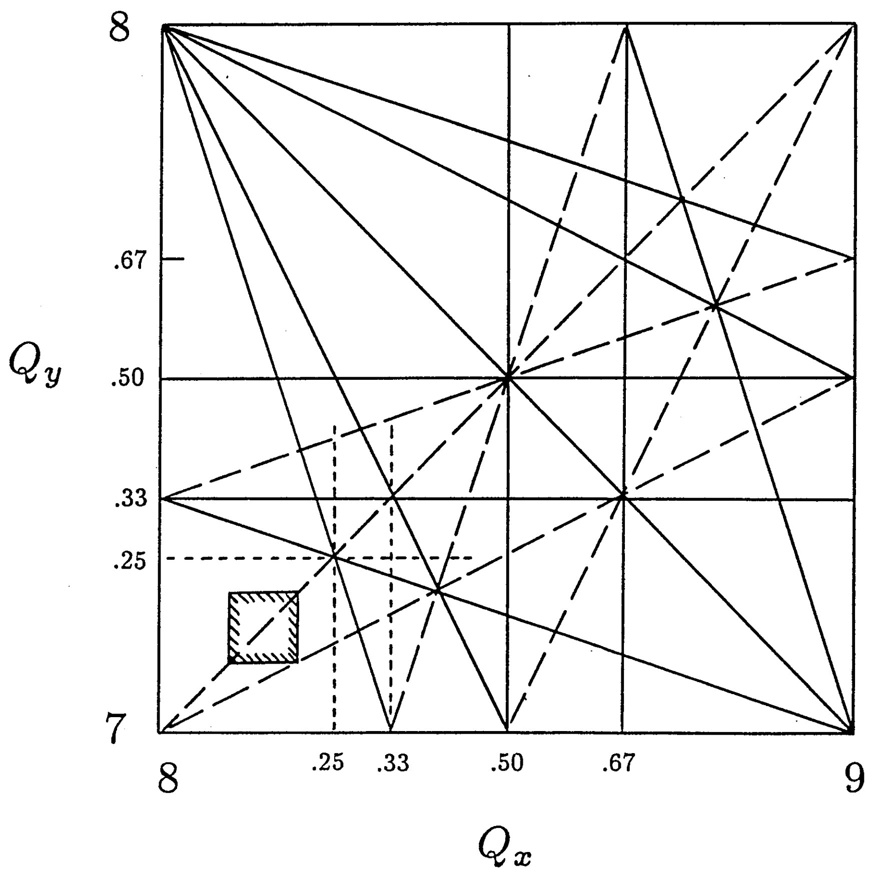

Figure 5. LISS betatron resonance lines through 4th order for periodicity 2. Square in lower left-hand corner denotes proposed working area.

Figure 5 shows the LISS betatron tune diagram, including all systematic resonances through 4th order for superperiodicity $P = 2$. Solid resonance lines denote possible instability or weak quasi-stability (beam loss); long dashes indicate strong quasi-stability (difference resonances, no beam loss); short dashes represent excitable 3rd and 4th order resonances in the vicinity of the working area (square in lower left-hand corner) which would be present in the absence of a true periodicity of 2.

III. *Polarized Beam Acceleration in LISS*

One of the principal purposes of LISS is to accelerate and store beams of highly polarized protons and deuterons. The preservation of polarization during acceleration is thus a crucial aspect of the LISS design.

In a circular accelerator the spin vector will precess about the vertical axis through $G\gamma$ turns per orbital revolution, where for protons $G = 1.79285$ and $\gamma = 1{+}T(\mathrm{GeV})/0.93827$. When this spin precession frequency equals the frequency ν_s of the spin-perturbing kicks, $G\gamma = \nu_s$, the beam polarization may be lost due to coherent addition of these kicks. The most dangerous depolarizing resonances are the linear resonances (of first order in betatron amplitude) due to horizontal-focussing magnetic fields encountered during vertical betatron oscillations.

The spin resonancy tune ν_s is given by $\nu_s = nP \pm \nu_y$ for linear "intrinsic" resonances and by $\nu_s = k$ for "imperfection" resonances, where n, k are integers, P the superperiodicity of the accelerator, and ν_y the transverse betatron tune (in a particle reference frame where x is radially outward, y vertically upward, and z longitudially forward). Intrinsic resonances arise from vertical betatron motion, and imperfection resonances arise from vertical closed-orbit distortions. In the present LISS racetrack lattice design, $P = 2$ and $\nu_y = 7.20$.

Over the energy range 0.4 GeV $\leq T \leq$ 15 GeV assumed here for a generic LISS, we have $1.43 \leq \gamma \leq 17$ and hence a large number (27) of intrinsic depolarizing resonances. The strengths (*i.e.* characteristic widths) of all intrinsic resonances encountered in LISS were computed for an emittance equal to half the ring acceptance and are plotted *vs.* γ in Fig. 6.

For the numerous integer (imperfection) resonances, the most important harmonic for the spin closed orbit is $k = \pm\, m$, where m is the integer closest to ν_y; here $m = 7$. Hence, the strongest imperfection resonances in LISS occur for $\nu_s = G\gamma = nP \pm m = 2n \pm 7 =$ odd-integer. Estimates of the maximum strengths of these imperfection-resonances were made for LISS, assuming an rms closed-orbit displacement of $\pm$ 2 mm; we find maximum values ranging from $\sim 8 \times 10^{-4}$ at injection to $\sim 7 \times 10^{-3}$ at 15 GeV.

For a fast-cycling synchrotron, the strongest spin resonances tend to be the most dangerous ones. Not so for a very slow ramping machine like LISS, where corrective steps need to be taken primarily in passing through resonances whose strength falls in the range $10^{-4} \leq \epsilon \leq 3 \times 10^{-3}$; this range encompasses all but the six strongest intrinsic resonances as well as most of the imperfection resonances.

To accelerate polarized protons through spin depolarizing resonances in LISS, the polarization can be maintained by (1) minimizing imperfection-resonance strengths to $< 10^{-4}$, (2) passing through a resonance slowly for adiabatic spin-flip, (3) passing through a resonance fast for non-adiabatic spin tune jump, or (4) using spin rotators called "snakes" to change the spin tune to a value which avoids spin resonances altogether.

Method (2) can be used to cross depolarizing resonances of strength ϵ provided the acceleration rate is $< \epsilon^2$ GeV/turn. For LISS the energy gain per turn is $\sim 10^{-5}$ GeV, slow enough for adiabatic spin-flip with >99% efficiency for $\epsilon > 3 \times 10^{-3}$; this level of resonance strength is indicated in Fig. 6 by the horizontal dashed line labeled "$\epsilon_{\rm min}$ for 99% spin flip." Method (3) has been used successfully in the ZGS, KEK, and AGS to overcome intrinsic resonances, but there are a number of undesirable side effects associated with sudden vertical betatron tune jumps that make this not the method of first choice. The preferred method (4), above, is to *avoid* all spin resonances (intrinsic as well as imperfection) altogether by use of a localized spin rotator which precesses the spin vector about an axis in the horizontal plane through an angle $\phi = \pi$, causing the spin tune of the accelerator to become $\nu_s = 1/2$ (modulo an integer), independent of energy. Such a $\phi = \pi$ rotator is known as a "full snake."

A "partial snake," which rotates the spin through $\phi < \pi$, is equivalent to an imperfection resonance of strength $\epsilon_{eq} = \phi/2\pi$, and may be employed in eliminating the effect of accelerator imperfection resonances provided the imperfection strength due to the partial snake dominates the spin dynamics, i.e., $\epsilon_{\rm eq} >> \epsilon_{\rm imp}$; then complete spin flip occurs

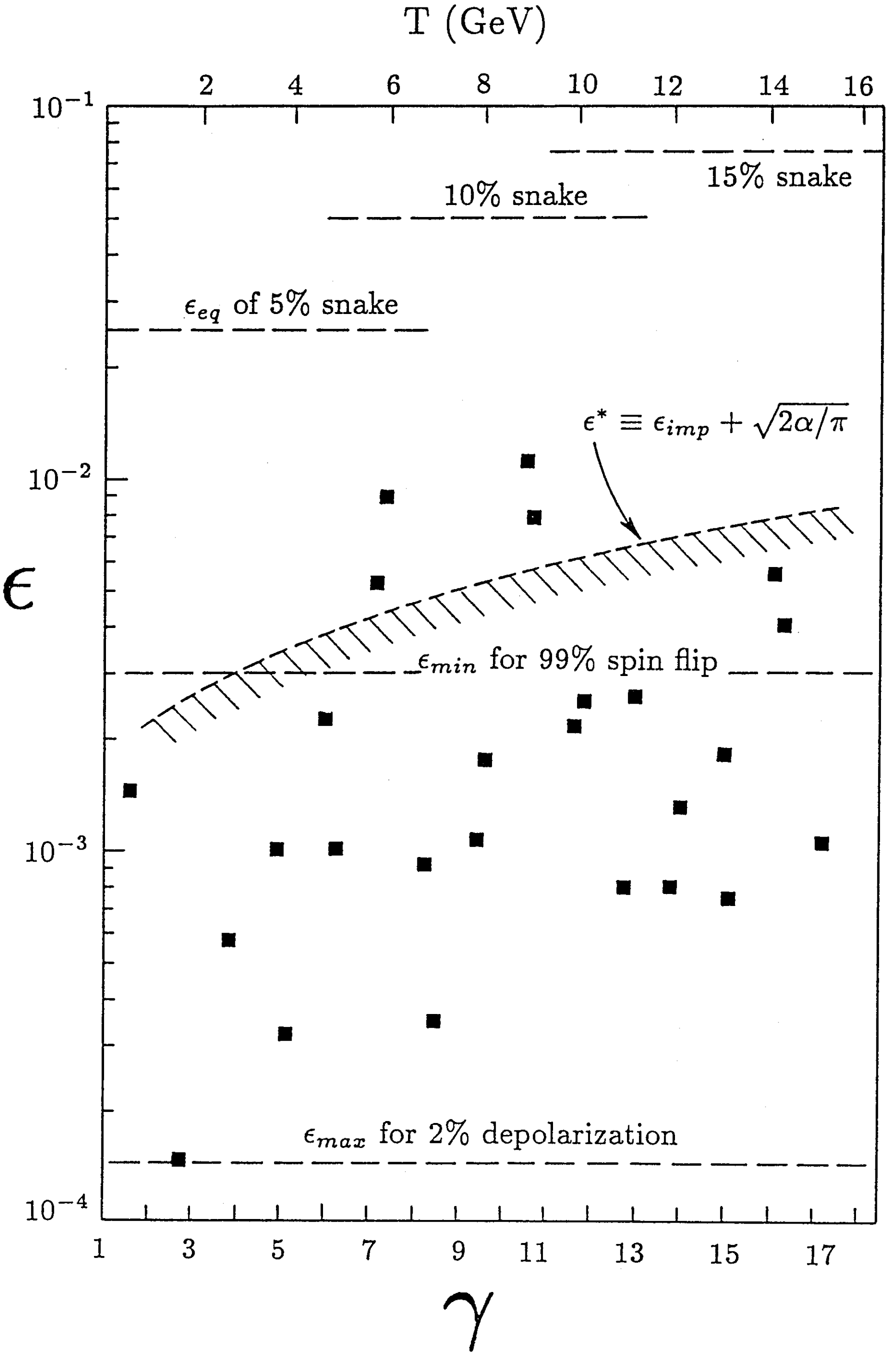

Figure 6. Strengths of all intrinsic (■) spin resonances for polarized protons in LISS. Adiabatic crossing of resonances with $\epsilon < 10^{-4}$ will result in $< 1\%$ depolarization; with $\epsilon > 3 \times 10^{-3}$ crossing will result in $> 99\%$ spin flip. Partial snakes with $\epsilon_{eq} \sim 10\epsilon^*$ will also produce complete spin flip at $G\gamma$ = integer resonances.

at each integer value of $G\gamma$. The required spin-rotation angle for the partial snake must satisfy $\phi >> 2\pi|\epsilon_{\text{imp}}| + \sqrt{8\pi\alpha} \equiv 2\pi\epsilon^*$ where $\alpha = (G/\omega_0)d\gamma/dt$ is the acceleration rate of the spin tune. For LISS, with $d\gamma/dt < 5$/s and orbit frequency $\omega_0 = 3 \times 10^6$/s, we have

$\alpha \leq 3 \times 10^{-6}$ and therefore, for the maximum values of $\epsilon_{\rm imp}$, we require a maximum value for the relative snake strength, $S \equiv \phi/\pi$, of about 0.15 ($S = 1$, or 100%, for a full snake). Figure 6 illustrates this relationship, showing $\epsilon_{\rm eq}$ for 5%, 10%, and 15% snakes in comparison to ϵ^* based on an upper limit to the expected imperfection-resonance strengths in LISS.

For LISS, use of the following options represents one possible scenario for maintaining essentially full proton beam polarization during acceleration:

(1) For energies up to $\sim$ 5 GeV, the combination of a <u>fixed</u> superconducting solenoid (13 T·m) and a <u>ramped</u> warm solenoid (0–9 T·m) provides a full snake to avoid the intrinsic resonances and overcome the imperfection resonances. A drawback of this type of full snake is the resulting strong coupling of horizontal and vertical phase spaces.

(2) For energies in the range of 5 – 10 GeV, the 4 strong instrinsic resonances near 6 and 9 GeV (cf. Fig. 6) are traversed with adiabatic spin flip (with $<$ 0.1% depolarization per flip for $\epsilon > 4 \times 10^{-4}$). The 4 weak intrinsic resonances between 6.8 and 8.3 GeV are safely crossed in fast passage via betatron tune jumps (using fast pulsed quadrupoles) or via spin tune jumps (using a fast partial snake). The imperfection resonances would be handled by a 10% partial snake.

(3) For acceleration to energies beyond $\sim$ 10 GeV, adiabatic turn-on of a ramped, helical-dipole full snake would avoid all intrinsic and imperfection resonances. A suitable helical dipole with continuous helical pitch (for smallest maximum orbit excursion in the magnet) could be achieved by twisting either a laminated warm dipole (under study at IHEP, Protvino, for the proposed Fermilab Tevatron polarized beam project) or a superconducting cosine dipole (under study at BNL for RHIC); the latter is more compact but applicable to LISS only if the turn-on time is measured in seconds, not minutes.

Finally, some comments about polarized deuteron acceleration in LISS. The deuteron gyromagnetic ratio, G =–0.1427, is about 13 times smaller than for the proton. For maximum momentum, p = 16 GeV/c, the maximum deuteron kinetic energy is 14.2 GeV, corresponding to a maximum $\gamma = 8.6$. Consequently, few if any spin resonances fall into this energy region: no intrinsic resonance, and only one $G\gamma = 1$ imperfection resonance at $\gamma = 7.0$ with an estimated strength of $\epsilon \sim 3 \times 10^{-4}$. For adiabatic spin-flip at this resonance, due to the low spin tune acceleration rate of $\alpha \leq 1.2 \times 10^{-7}$, a 1% snake (S=0.01) should suffice.

IV. *Ring Magnets*

A preliminary magnetic and conceptual engineering design of all racetrack lattice dipoles and quadrupoles was carried out to the extent of allowing us to make reasonably realistic cost estimates for magnet fabrication, power supplies, AC power installation, and cooling-water systems.

The present lattice design, e.g., choice of FODO cell size, is based on the use of warm (normal-conducting) magnets. This choice was made because (1) it lowers LISS construction costs (installation cost of warm magnets and associated power supplies for a $\leq$ 20-GeV synchrotron is significantly less than that of superconducting magnets and associated liquid helium refrigeration systems), and (2) the required total bending magnet length for a 16-GeV/c synchrotron at 1.7 T peak dipole field is not yet excessive (about 200 m, or 1/3 of the ring circumference).

Full beam-stay-clear apertures for LISS arc magnets are 6 cm V × 8 cm H. Physical magnet apertures (with 1-cm allowance for beam pipes) are 7.0-cm pole gaps for dipoles and 3.5-cm (4.5-cm) bore radius for quadrupoles in the arcs (long straight sections).

The LISS racetrack lattice incorporates 36 arc dipoles (28 × 11.25° nominal bend angle each, 6.16-m long with $B_{\max} = 1.7$ T; plus 8 shorter dipoles in the dispersion-suppressor cells) and 80 quadrupoles of various strengths ($kL = 0.1$ - 0.4 m^{-1}). Some number (still to be determined) of chromaticity-correcting sextupoles and small dipole orbit correctors are also needed.

All ring magnets, along with their associated power supplies, are designed to be ramped, with a 3 s minimum upramp (maximum dipole field ramprate ~ 0.5 T/s). All magnets will have steel cores assembled from stamped, 16 gauge, low-carbon steel laminations. Dipoles will be of conventional H-frame design with recessed (out of midplane) coil windows accommodating flat coils.

V. *Electron Cooling System*

At 10^{12} particles in the ring, cooling of the beam phase space at or near the injection energy in LISS would lead to severe space-charge problems. Beam cooling at the high end of the LISS energy range would be very slow (by stochastic cooling) or very expensive (by electron cooling). In the energy range between roughly 2.5 and 5 GeV, however, electron cooling can (1) significantly reduce the beam emittance without exceeding conservative space charge tune shift limits, and (2) do so with available and affordable technology.

At the electron energy of roughly 1.4 to 2.7 MeV required for cooling 2.5 to 5 GeV proton beams, the traditional approach of using an open-air Cockcroft-Walton high-voltage terminal to generate and collect a multi-ampere, magnetically-confined electron beam is impractical. Instead, a non-magnetically-confined electron beam generated and collected in the terminal of a multi-MV, dual-acceleration column ("Pelletron") DC accelerator appears to be the most suitable technology for intermediate-energy electron cooling systems. This electron recirculation technology has already been demonstrated to some degree, and further development to the required performance level appears technically feasible. The remaining technical issues will likely be resolved in the near future by development of a 5-MeV electron system at Fermilab for cooling 8-GeV antiprotons in a new "recycler" ring.

Using reasonable values for the electron cooling system parameters, transverse emittance damping times $\tau_{1/e}$ ranging from 4 to 20 s were computed for 2.5 to 5-GeV proton beams of normalized initial emittance $\epsilon_N = 1\ \pi\ \mu$m and rms momentum spread $\Delta p = \pm\ 6$ MeV/c, assuming an average radial aperture function $\langle\beta\rangle = 9$ m in the cooling region of length $L_C = 12$ m (a fraction $\eta = 2\%$ of the ring circumference). These 1/e cooling times can be halved by halving the initial ϵ_N, and nearly halved again by, in addition, doubling $\langle\beta\rangle$ (the original value of 9 m for $\langle\beta\rangle$ is predicated on using one of the six standard, low-β experimental straight sections in LISS for electron cooling, and modification of the LISS optics to increase $\langle\beta\rangle$ locally in the electron cooling section would not be too difficult). These cooling-time results are displayed as a function of proton energy,

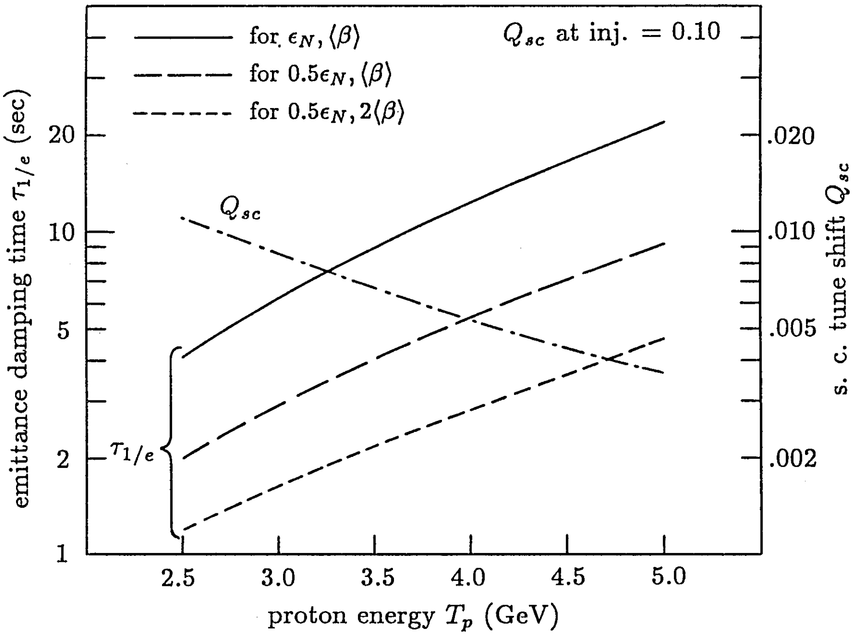

Figure 7. Transverse cooling times as function of proton energy for various beam emittances ϵ_N and cooling-section average beta functions. Also shown is the space-charge tune shift Q_{sc} before cooling, assuming Q_{sc} = 0.1 at injection.

T_p, in Fig. 7, for an electron current of 2 A. Also shown in Fig. 7 is the space-charge tune shift Q_{sc} before cooling, assuming $Q_{sc} = 0.1$ at injection.

Specifically, using a 2-MV Pelletron for recirculating a 2-MeV/2-A electron beam, electron cooling at $T_p \approx 3.7$ GeV to produce an order-of-magnitude reduction in the transverse beam emittance with characteristic cooling times $\tau_{1/e} \sim 2$ to 5 s, or $\tau_{1/10} \sim 3$ to 8 s, is a realistic goal. Electron cooling at this proton energy is almost 2 orders of magnitude faster than stochastic cooling of 10^{12} particles. With a cooling time scale of the same order as the LISS acceleration ramp time, a ramp-cool-ramp approach to final proton energies greater than 3.7 GeV is entirely reasonable.

1. S.Y. Lee, *et al.*, Phys. Rev. E **48**, 3040 (1993).